Chemical Physics Impact 9 (2024) 100712

Contents lists available at ScienceDirect

Chemical Physics Impact

journal homepage: www.sciencedirect.com/journal/chemical-physics-impact

Full Length Article

Investigation of antibacterial and antifungal properties of benzene sulfonamide derivatives by experimental and computational studies

Özge Kapısuz [a], Mithun Rudrapal [b,*], Ülküye Dudu Gül [c], Sanket S. Rathod [d], Mesut Işık [c,*], Mustafa Durgun [e], Johra Khan [f]

[a] Department of Bioengineering, Graduate School of Education, Bilecik Seyh Edebali University, Bilecik, Turkey
[b] Department of Pharmaceutical Sciences, School of Biotechnology and Pharmaceutical Sciences, Vignan's Foundation for Science, Technology & Research, Guntur, Andhra Pradesh, India
[c] Department of Bioengineering, Faculty of Engineering, Bilecik Seyh Edebali University, Bilecik, Turkey
[d] Department of Pharmaceutical Chemistry, Bharati Vidyapeeth College of Pharmacy, Kolhapur, Maharashtra, India
[e] Department of Chemistry, Faculty of Arts and Sciences, Harran University, Şanlıurfa, Turkey
[f] Department of Medical Laboratory Sciences, College of Applied Medical Sciences, Majmaah University, Al Majmaah, Saudi Arabia

ARTICLE INFO

Keywords:
Benzene sulfonamide
Antibacterial
Antifungal
Molecular docking
In-silico drug-likeness

ABSTRACT

This study investigates the antibacterial and antifungal properties of eight benzene sulfonamide derivatives synthesized and reported in our previous study using a combination of experimental and computational methods. In antimicrobial activity, the MIC values of all the eight tested compounds were approximately 125.00 μg/mL against eight bacterial and three fungal strains. However, the compound **8** was found to exhibit remarkable activity (MIC=31.25 μg/mL) against *E. faecalis* (bacteria) and *C. parapsilosis* (fungi) compared to the MIC values of rest of the compounds. Results of *in-silico* drug-likeness and pharmacokinetic (ADMET) assessment reveal that all the title compounds met the compliance of criteria of drug-likeness rules and exhibited zero violations across. Results of docking study demonstrates that the compound **8** showed the highest binding affinity (-8.7 kcal/mol) among the compounds against *S. aureus* TyrRS, whereas against *S. aureus* DHFR, compound **2** exhibited the highest binding afinity of -8.5 kcal/mol. Among the compounds docked against *C. albicans* DHFR and *C. albicans* N-myristoyl transferase, compound **8** demonstrated the highest binding affinity of -8 kcal/mol and -8.9 kcal/mol, respectively. The results of antibacterial and antifungal experiments substantiate the predictions made by computational studies and provide empirical evidence of antibacterial and antifungal potential of the reported benzene sulfonamide derivatives.

1. Introduction

Sulfonamides are widely used as antimicrobial agents for therapeutic purposes in human and animal health. Drugs belonging to the sulphonamide class revolutionized medicine and organic chemistry because of their medicinal properties ranging from antibacterial to anti-inflammatory properties. Because of their therapeutic and beneficial properties, organic chemists have developed new synthetic methods for sulfonamides, and as newer methodologies have established, many sulfonamide derivatives have been synthesized in the past [1,2].

Organic Schiff bases derived from azomethine are formed by a simple condensation of primary amines and carbonyl compounds under slightly acidic conditions. Schiff bases are important reaction intermediates often incorporated into heterocyclic scaffolds of medicinal or pharmaceutical interest. Oxygen-, nitrogen-, and sulfur-containing heterocycles exhibit significant biological and microbiological activities that are often found in bioactive natural products, synthetic drug molecules, and organic pharmaceutical compounds. The selection of heterocyclic building scaffolds is the key component in new drug design strategy which has gained remarkable interest in medicinal chemistry and drug discovery research. The synthetic heterocyclic derivatives have been reported to exhibit many pharmacological activities, such as antibacterial, anti-inflammatory, antioxidant, and antiviral [3,4]. However, a nitrogen atom of azomethine can form hydrogen bonding by donating lone electron pairs with active cellular components, interrupting the normal function of bacterial cells. Moreover, sulfonamides are desirable

* Corresponding authors.
E-mail addresses: rsmrpal@gmail.com, drmr_pharma@vignan.ac.in (M. Rudrapal), mesut.isik@bilecik.edu.tr (M. Işık).

https://doi.org/10.1016/j.chphi.2024.100712
Received 15 June 2024; Received in revised form 10 August 2024; Accepted 16 August 2024
Available online 17 August 2024

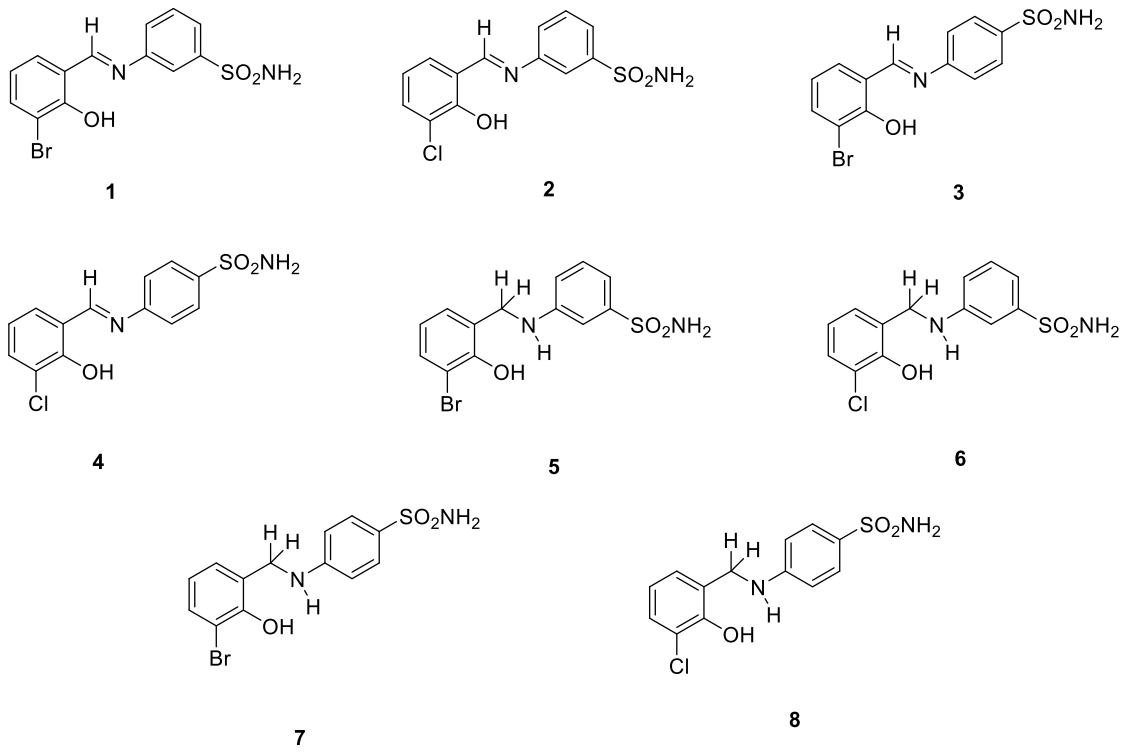

Fig. 1. Chemical structures of compounds under investigation.

pharmacophores that are widely used in many drug development processes; they are used as adjuvants to other antibiotics for the treatment of many bacterial infections. Furthermore, the use of the sulfonamide functional group in several heterocyclic rings has been widely applied for drug discovery, and the resulting derivatives have reported antibacterial, antiviral, anticancer, anticonvulsant and antifungal activities [5–7].

Drug resistance is an important factor in antimicrobial studies. Therefore, it is extremely important to understand the mechanism of inhibition through computational such as molecular docking and experimental studies. Molecular docking is a molecular modeling technique used to determine the orientation and interaction (hydrogen bonding, electrostatic, van der Waals, etc.) of a drug molecule when binding with biomolecules such as receptors, enzymes, proteins or DNA. Computational studies help to investigate the physicochemical properties and binding patterns of synthesized compounds and offer insights into their antibacterial and antifungal potential. The current study employs molecular docking to predicting the binding affinity of these compounds against specific antibacterial or antifungal protein targets, validating the experimental results [1,8]. The study investigates the antibacterial and antifungal potential of sulfonamide Schiff bases, synthesized in our previous study [9], using experimental and computational methods.

2. Material and methods

2.1. Antimicrobial assays

Experimental details, data, and spectral analyses of synthesized sulfonamide Schiff bases were presented in our previous published reports [9]. The antimicrobial activity of final compounds was screened on eight bacterial and three fungal strains according to the standard procedure of Clinical & Laboratory Standards Institute (CLSI) [10,11] as described in the previous study [12]. The antibacterial activities were tested against *Escherichia coli* (ATCC 25,922), *Serratia marcescens* (ATCC 8100), *Klebsiella pneumoniae* (ATCC 13,883), *Pseudomonas aeruginosa* (ATCC 27,853), *Enterococcus faecalis* (ATCC 2942), *Bacillus subtilis* (ATCC 6633), *Staphylococcus aureus* (ATCC 29,213), and *Staphylococcus epidermidis* (ATCC 12,228). *Candida albicans* (ATCC 24,433), *Candida krusei* (ATCC 6258), and *Candida parapsilosis* (ATCC 22,019) were used to test the antifungal activity of the same compounds. Azithromycin and tetracycline (against bacterial strains) and fluconazole and voriconazole (against candida strains) were used as standard reference drugs. The assays were carried out in triplicate in two different time periods. The average of MIC values was evaluated. Results are shown as means ± of standard error of mean (SEM) of three replicate observations ($n = 3$). The statistical difference between the groups for MIC values was calculated by two-way ANOVA followed by Tukey's multiple comparison post hoc test. Values with $p < 0.05$ were considered statistically significant. The statistical software program (GraphPad Prism 8) was used for the analysis of results.

2.2. Computational methods

2.2.1. Ligand preparation

The chemical structures of synthesized compounds (**1**–**8**) (Fig. 1) were sketched utilizing ACD/ChemSketch software [13,14]. Hydrogen atoms were added using BIOVIA Discovery Studio [15]. The prepared ligand structures were then energy minimised and optimised using MMFF94 force field along with the steepest descent algorithm [16]. The ligand preparation protocol was done employing the Open Babel module from PyRx 0.8 [17].

2.2.2. In-silico drug-likeness and ADMET assessment

The theoretical drug-likeness and pharmacokinetic (ADMET) parameters of the studied compounds was assessed as per previously reported protocol *via* the SwissADME and pkCSM servers [18,19].

2.2.3. Molecular docking study

Previously reported 3D crystal structure of *S. aureus* tyrosyl-

Table 1
Antibacterial activity of compounds, 1–8 as MIC values (μg/mL).

Compound	A	B	C	D	E	F	G	H
1	125 ± 0.12	125 ± 0.42	125 ± 0.18	125 ± 0.21	62.5 ± 0.16*	125 ± 0.42	125 ± 0.21	125 ± 0.34
2	125 ± 0.11	125 ± 0.51	125 ± 0.56	125 ± 0.10	125 ± 0.28	125 ± 0.26	125 ± 0.19	125 ± 0.17
3	125 ± 0.23	125 ± 0.16	125 ± 0.24	125 ± 0.22	125 ± 0.31	125 ± 0.34	125 ± 0.42	62.5 ± 0.11*
4	125 ± 0.24	125 ± 0.29	125 ± 0.15	125 ± 0.47	125 ± 0.56	125 ± 0.24	125 ± 0.33	62.5 ± 0.12*
5	125 ± 0.16	125 ± 0.22	125 ± 0.18	125 ± 0.20	125 ± 0.25	125 ± 0.16	125 ± 0.41	125 ± 0.12
6	125 ± 0.56	62.5 ± 0.31*	125 ± 0.42	125 ± 0.17	125 ± 0.67	125 ± 0.30	125 ± 0.17	125 ± 0.33
7	125 ± 0.19	62.5 ± 0.17*	125 ± 0.32	125 ± 0.49	125 ± 0.14	125 ± 0.42	125 ± 0.31	125 ± 0.51
8	125 ± 0.23	125 ± 0.17	125 ± 0.10	125 ± 0.28	31.25 ± 0.12*	125 ± 0.20	125 ± 0.32	125 ± 0.32
SD1	< 0.97 ± 0.19	< 0.97 ± 0.16	< 0.97 ± 0.28	< 0.97 ± 0.31	< 0.97 ± 0.47	< 0.97 ± 0.45	< 0.97 ± 0.12	< 0.97 ± 0.67
SD2	7.81 ± 0.21	3.91 ± 0.23*	7.81 ± 0.32	31.25 ± 0.44	15.63 ± 0.24*	7.81 ± 0.56	0.97 ± 0.41	62.5 ± 0.20*

* : Most active compounds. **A:** *E. coli* (ATCC 25,922), **B:** *S. marcescens* (ATCC 8100), **C:** *K. pneumoniae* (ATCC 13,883), **D:** *P. aeruginosa* (ATCC 27,853), **E:** *E. faecalis* (ATCC 2942), **F:** *B. subtilis* (ATCC 2478), **G**: *S. aureus* (ATCC 29,213), **H:** *S. epidermidis* (ATCC 12,228) **A-D:** Gram-negative bacteria, **E-H:** Gram-positive bacteria. **SD1** (Standard drug): Azithromycin; **SD2 (**Standard drug): Tetracycline. Data are given as mean ± SEM, $n = 3$. * indicates means between the groups differ significantly at the level of $p < 0.05$.

Table 2
Antifungal activity of compounds, 1–8 as MIC values (μg/mL).

Compound	A	B	C
1	250 ± 0.24	125 ± 0.32	62.5 ± 0.11*
2	250 ± 0.21	125 ± 0.44	62.5 ± 0.13*
3	250 ± 0.23	125 ± 0.37	62.5 ± 0.32*
4	>250 ± 1.20	125 ± 0.52	62.5 ± 0.16*
5	>250 ± 0.25	125 ± 0.24	125 ± 0.22
6	>250 ± 1.11	125 ± 0.92	125 ± 1.11
7	>250 ± 1.10	125 ± 0.34	125 ± 0.23
8	>250 ± 1.11	125 ± 0.16	31.25 ± 0.52
SD1	3.90 ± 0.24	3.90 ± 0.34	1.95 ± 0.45*
SD2	7.81 ± 0.24	7.81 ± 0.23	3.90 ± 0.24*

* : Most active compounds. **A:** *C. albicans* (ATCC 24,433), **B:** *C. krusei* (ATCC 6258), **C:** *C. parapsilosis* (ATCC 22,019*)*. **SD 1** (Standard drug 1): Voriconazole, **SD2** (Standard drug2): Fluconazole. Data are given as mean ± SEM, $n = 3$. * indicates means between the groups differ significantly at the level of $p < 0.05$.

tRNAsynthetases (TyrRS) (PDB: 1JIJ, resolution 3.20 Å), *S. aureus* dihydrofolate reductase (DHFR) (PDB: 3FYV, resolution 2.20 Å), *C. albicans* DHFR (PDB: 4HOF, resolution 1.76 Å), and *C. albicans* N-myristoyltransferase (PDB: 1IYL, resolution 3.20 Å) were retrieved in PDB format from the RCSB Protein Data Bank for the docking study [20–24]. Protein structures were then underwent to refinement following removal of the previously bounded water and hetero atoms from all the selected PDB files. Polar hydrogen atoms were added in each protein structure to correct tautomeric and ionization states of amino acid residues [25,26]. BIOVIA Discovery Studio was used to carry out protein refinement step [15,27]. The prepared protein structures were energy-minimized on PyRx 0.8 with converting into AutoDock macromolecules for further investigation.

The molecular docking of the compounds was performed against selected bacterial and fungal molecular targets described above employing AutoDockVina module of PyRx 0.8 [28,29]. The one-by-one energy minimised structures of selected proteins and all the ligands were selected in Vina Wizard. Each time a maximised grid box was selected to cover entire protein structure for docking study utilizing blind docking approach [30]. The exhaustiveness parameter for docking was set default at eight to control conformational states of docked ligand [31]. Finally, the docked binding conformations for each ligands with the highest binding affinity (BA) was saved for further analysis. BIOVIA Discovery Studio was used to visualize binding interactions of docked ligands with the targeted proteins.

3. Result and discussion

3.1. Antibacterial activity

The results of antibacterial activity are presented in Table 1. Generally, the MIC values were approximately 125.00 μg/mL for almost all the studied compounds. However, compound **8** was found to be the most active (31.25 μg/mL) against *E. faecalis* compared to the MIC

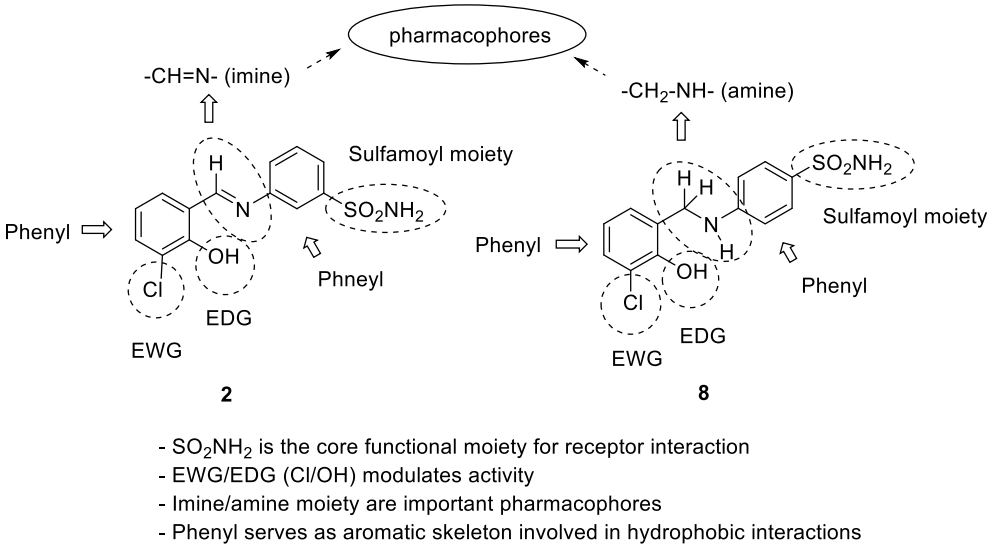

Fig. 2. SARs of newer benzene sulphonamide analogues.

Table 3
Predicted physicochemical and drug-likeness properties of compounds.

Compound	MW (g/mol)	mLogP	HBA	HBD	MR	TPSA	nRot	Lipinski's Rule (Ro5)	Veber's Rule	Ghose's Rule	Egan's Rule	Muegge's Rule
1	355.21	1.63	5	2	80.86	101.13	3	+	+	+	+	+
2	310.76	1.5	5	2	78.17	101.13	3	+	+	+	+	+
3	355.21	1.63	5	2	80.86	101.13	3	+	+	+	+	+
4	310.76	1.5	5	2	78.17	101.13	3	+	+	+	+	+
5	357.22	1.71	4	3	80.95	100.8	4	+	+	+	+	+
6	312.77	1.58	4	3	78.26	100.8	4	+	+	+	+	+
7	357.22	1.71	4	3	80.95	100.8	4	+	+	+	+	+
8	312.77	1.58	4	3	78.26	100.8	4	+	+	+	+	+

values of other compounds. Compounds **1, 3** and **4** and **6** and **7** showed better activity (62.5 μg/mL) against *E. faecalis, S. epidermidis* and *S. marcescens,* respectively as compared to rest of the analogues. When results are examined, it is observed that all tested compounds act similarly against gram-positive (+) and gram-negative (-) strains. The activity of test compounds was of course less than that of the standard drugs, azithromycin and tetracycline.

3.2. Antifungal activity

The MIC values of the tested compounds against *Candida* strains are given in Table 2. The compounds 8 was found to be the most active against *C. parapsilosis* with MIC value of 31.25 μg/mL comparing the MIC values of other compounds. Compounds 1–4 exhibited somewhat better activity (62.5 μg/mL) compared to rest of the compounds. However, the antifungal activities of the two standard drugs (voriconazole and fluconazole) were more active than the tested compounds.

From overall results it is clear that all the sulfonamide Schiff bases possess superior antibacterial effectiveness than antifungal activity. The compound **8** was found to be the most active against both bacterial and fungal strains. The results of our study concord several previous studies where sulphonamides, sulfonyl hydrazones and benzene sulfonamides have been reported to exhibit antibacterial and antifungal activities with promising MIC values against a range of gram-positive and gram-negative organisms such as *S. aureus, B. subtilis, E. coli, P. aeruginosa, C. albicans* and *A. niger* [32,1,33]. Fig. 2 illustrates the structure-activity relationships of newly reported benzene sulphonamide analogues taking compound **2** and compound **8** as the prototype molecules as they are the most active compounds among eight analogues. Both the analogues are structurally similar to each other expect for the key pharmacophoric imine or amine moiety. The compound **8** possess better activity than the compound **2**, which might be because of more stability of the amine functionality over the imine moiety. The presence of electron withdrawing group (EWG, example, -Cl) and electron donating group (EDG, example, -OH) in the phenyl ring and their correct position (*ortho* to each other) are also considered to be important for the activity, which may modulate the potency if the nature of groups and their relative positions change. The phenyl ring with the sulfamoyl moiety is believed to be the core functional moiety responsible for direct interaction with the receptor molecule.

3.3. In-silico drug-likeness and ADMET assessment

The present study encompasses an exhaustive evaluation of the physicochemical properties of the synthesized compounds to ascertain their drug-likeness and potential pharmacokinetic profiles. This estimation helped to investigate drug-likeness profiles of the title compounds considering established rules such as Lipinski's Rule (Ro5), Veber's Rule, Ghose's Rule, Egan's Rule, and Muegge's Rule [34,35]. These rules serve as guidelines for identifying favourable drug-likeness properties of compounds. Remarkably, all the compounds, **1–8** successfully met the criteria outlined in this drug-likeness rules and exhibited zero violations across the spectrum of criteria. The evaluation unveiled that a majority of the compounds demonstrated compliance with these selected drug-likeness rules. This outcome intensifies the understanding of the potential suitability of title compounds for further essential optimization. Table 3 represents the predicted physicochemical properties and drug-likeness profile of compounds, **1–8**.

The pharmacokinetic profiling of the compounds, **1–8** was carried out using the pkCSM server to estimate their ADMET properties. The information pertaining to predicted ADMET properties of the compounds, **1–8** is detailed in Table 4. A noteworthy observation emerged from this analysis and revealed the promising nature of intestinal absorption of each compound surpassing the threshold of 77%. Specifically, the range of intestinal absorption for these compounds varied between 77.01% and 82.08%. Among the synthesized compounds, compound **2** and **4** exhibited the highest percentage of intestinal absorption. Nevertheless, it is important to admit that further optimization of their physicochemical and structural properties are warranted to achieve their increased intestinal absorption capabilities. The

Table 4
Predicted pharmacokinetic (ADMET) properties of compounds.

Compound	Absorption	Distribution			Metabolism							Excretion	Toxicity	
	Intestinal absorption (human)	VDss (human)	BBB permeability	CNS permeability	Substrate		Inhibitors					Total clearance	AMES toxicity	Hepatotoxicity
					CYP									
					2D6	3A4	1A2	2C19	2C9	2D6	3A4			
	Numeric (% absorbed)	Numeric (log L kg^{-1})	Numeric (log BB)	Numeric (log PS)	Categorical (Yes/No)							Numeric (log mL min^{-1} kg^{-1})	Categorical (Yes/No)	
1	81.81	−0.22	−0.39	−2.29	No	Yes	Yes	No	No	No	No	−0.11	No	No
2	82.08	−0.23	−0.38	−2.31	No	Yes	No	No	No	No	No	0.07	No	No
3	81.81	−0.22	−0.37	−2.29	No	Yes	Yes	No	No	No	No	−0.17	No	No
4	82.08	−0.23	−0.36	−2.31	No	Yes	No	No	No	No	No	0.01	No	No
5	77.01	−0.32	−0.93	−2.50	No	No	No	No	No	No	No	−0.22	No	No
6	77.28	−0.33	−0.91	−2.52	No	No	No	No	No	No	No	−0.04	No	No
7	77.01	−0.33	−0.93	−2.50	No	No	No	No	No	No	No	−0.29	No	No
8	77.28	−0.34	−0.91	−2.52	No	No	No	No	No	No	No	−0.11	No	No

Table 5
Binding interactions and affinities of sulfonamide Schiff bases against bacterial molecular targets.

Comp.	*S. aureus* TyrRS (PDB: 1JIJ)				*S. aureus* DHFR (PDB: 3FYV)			
	BA	Interacting residue	Type of interaction	Distance	BA	Interacting residue	Type of interaction	Distance
1	−7.4	Lys84	Conventional H Bond	2.19	−8.3	Asn18	Conventional H Bond	1.95
		His50	Conventional H Bond	2.20		Leu5	Alkyl, π-Alkyl	3.99
		Asp195	π-Anion	3.58		Phe92	Alkyl, π-Alkyl	4.50
		His50	π -π T-Shaped	5.15		Val31	Alkyl, π-Alkyl	4.10
		Leu70	Alkyl	5.17		Ile14	Alkyl, π-Alkyl	5.26
						Leu20	Alkyl, π-Alkyl	5.11
2	−7.8	Asp195	Conventional H Bond	2.20	−8.5	Asn18	Conventional H Bond	2.48
		Asp40	Conventional H Bond	2.78		Leu20	Alkyl, π-Alkyl	5.16
		Asp177	Halogen (Cl, Br, I)	3.00		Phe92	Alkyl, π-Alkyl	4.37
		Asp195	π-Anion	3.68		Leu5	Alkyl, π-Alkyl	3.99
		Leu70	Alkyl	5.26		Val31	Alkyl, π-Alkyl	4.09
						Ile14	Alkyl, π-Alkyl	5.21
3	−8	Asp40	Conventional H Bond	2.27	−8.1	Phe92	Conventional H Bond	2.09
		Gln174	Conventional H Bond	2.86		Asn18	Conventional H Bond	2.05
		Gly38	C-H Bond	3.54		Thr46	π -Donor H Bond	3.12
		Asp195	π-Anion	3.47		Phe92	π -π Stacked	4.51
		Pro53	π-Alkyl	5.41		Leu5	Alkyl, π-Alkyl	4.08
		His47	π-Alkyl	4.88		Val31	Alkyl, π-Alkyl	4.17,5.41
		His50	π-Alkyl	4.63		Ile14	Alkyl, π-Alkyl	5.44
						Leu20	Alkyl, π-Alkyl	5.19
						Phe92	Alkyl, π-Alkyl	4.67
4	−8.1	Gly38	Conventional H Bond	2.82	−8.2	Thr46	π -Donor H Bond	3.17
		Asp177	Conventional H Bond	2.56		Phe92	π -π Stacked	4.45
		Gln174	Conventional H Bond	2.56		Ile14	Alkyl, π-Alkyl	5.35
		Asn124	Conventional H Bond	2.60		Val31	Alkyl, π-Alkyl	4.17,5.25
		Asp195	π-Anion	3.78		Leu5	Alkyl, π-Alkyl	4.02
		Pro53	Alkyl, π-Alkyl	3.72		Leu20	Alkyl, π-Alkyl	5.31
		His50	Alkyl, π-Alkyl	4.46		Phe92	Alkyl, π-Alkyl	4.50
5	−8.5	Gln174	Conventional H Bond	2.80	−8.3	Ile14	Conventional H Bond	2.11
		Thr75	Conventional H Bond	2.35		Gln95	Conventional H Bond	2.10
		Asp40	Conventional H Bond	1.98		Thr46	Conventional H Bond	2.59
		Asn124	Conventional H Bond	3.10		Asn18	Conventional H Bond	2.14
		Cys37	π -Sulfur	5.13		Gly94	C-H Bond	3.51
		-Pro53	π-Alkyl	5.27		Phe92	π -π T-Shaped	5.02
		His50	π-Alkyl	4.58		Leu20	Alkyl, π-Alkyl	5.45
						Ala7	Alkyl, π-Alkyl	3.97
						Val31	Alkyl, π-Alkyl	4.92
6	−8.5	Asp80	Conventional H Bond	2.84	−8.1	Ser49	Conventional H Bond	2.52
		Asp40	Conventional H Bond	1.96		Phe92	Conventional H Bond	2.45
		Gly38	Conventional H Bond	2.31		Leu5	Conventional H Bond	1.93
		Gln174	Conventional H Bond	1.97		Ala14	Conventional H Bond	2.15
		Gln196	Conventional H Bond	2.17		Ile14	C-H Bond	3.52
		Asp80	C-H Bond	3.30		Thr46	π -Donor H Bond	3.27
		Gln196	C-H Bond	3.33		Phe98	π -Sulfur	5.79
						Phe92	π -π T-Shaped	5.20
						Leu20	Alkyl, π-Alkyl	4.92
						Lys45	Alkyl, π-Alkyl	4.37
7	−7.7	Lys84	Conventional H Bond	2.04	−8.2	Ser49	Conventional H Bond	2.52
		Tyr170	Conventional H Bond	2.29		Thr46	Conventional H Bond	2.84
		Asp40	Conventional H Bond	1.88		Asn18	Conventional H Bond	1.92
		Asp80	C-H Bond	3.63		Ala7	Conventional H Bond	1.54, 3.07, 3.97
		His50	π-Sulfur	5.88		Thr46	π -Donor H Bond	3.04
		Lys84	π-Cation	4.47		Phe92	π -π T-Shaped	4.94
		Leu70	Alkyl, π-Alkyl	4.03		Val31	Alkyl, π-Alkyl	4.63
		Tyr36	Alkyl, π-Alkyl	5.49		Leu20	Alkyl, π-Alkyl	5.42
						Ala7	Alkyl, π-Alkyl	3.97
8	−8.7	Asp195	Conventional H Bond	2.83	−8.3	Thr121	Conventional H Bond	2.08
		Gln196	Conventional H Bond	2.70		Leu5	Conventional H Bond	2.01
		Asp40	Conventional H Bond	2.14		Phe92	Conventional H Bond	2.53
		Gln174	Conventional H Bond	2.79		Ala7	Conventional H Bond	2.36
		Pro53	Alkyl, π-Alkyl	4.32,4.69		Ile14	π-Alkyl	5.14
						Leu20	π-Alkyl	5.37

compounds exhibited promising predicted values for several key parameters essential for drug development. Specifically, assessments revealed favorable values concerning the volume of distribution in humans, blood-brain barrier (BBB) permeability, and central nervous system (CNS) permeability. These findings highlight the potential of achieving the adequate distribution of these compounds in the human body. However, in terms of metabolic interactions, it was observed that all compounds with the exception of compounds **1, 2, 3**, and **4** were identified as substrates of CYP3A4. CYP3A4 stands as a pivotal enzyme involved in drug metabolism which is important for potential interactions and considerations for their metabolic fate within the body. Furthermore, the assessments of AMES toxicity and hepatotoxicity for each compound were done as they are crucial facets of the safety evaluation. The results of ADMET prediction indicated a lack of AMES toxicity and hepatotoxicity associated with the target compounds. The positive results for AMES toxicity and hepatotoxicity assessment

Table 6
Binding interactions and affinities of sulfonamide Schiff bases against fungal molecular targets.

Comp.	*C. albicans* DHFR (PDB: 4HOF)				*C. albicans* N-myristoyl transferase (PDB: 1IYL)			
	BA	Interacting residue	Type of interaction	Distance	BA	Interacting residue	Type of interaction	Distance
1	−7.6	GLY114	Conventional H Bond	2.75	−8	ASP110	C-H Bond	3.58
		ARG56	Conventional H Bond	3.32		PHE240	π-Sulfur	5.60
		ARG79	Conventional H Bond	3.01		HIS227	π-π Stacked	4.74
		ARG79	π-Cation	4.49		PHE339	π-π Stacked	5.42
		GLU116	π-Donor H Bond	2.97		TYR354	π-π T-Shaped	5.00
		ALA115	π-Alky	4.60		TYR225	π-π T-Shaped	4.39
		LYS57	π-Alky	4.31,5.45		LEU415	Alkyl, π-Alky	4.75
		ARG56	π-Alky	5.68		LEU394	Alkyl, π-Alky	4.88
2	−7.3	SER61	Conventional H Bond	2.30	−7.9	THR211	Conventional H Bond	2.39
		GLY23	Conventional H Bond	2.93		ASN175	Conventional H Bond	2.25
		THR58	Conventional H Bond	2.57		LEU451	π-Anion	3.36
		GLY23	C-H Bond	3.34		LEU394	π-Sigma	3.96
		MET 25	π-Sigma	3.75		PHE117	π-π Stacked	5.15
		TYR118	π-π T-Shaped	5.87		TYR354	π-π T-Shaped	4.93
		ALA115	Alkyl, π-Alky	5.15		CYS393	Alky	5.27
		VAL10	Alkyl, π-Alky	5.22		LEU394	Alky	4.19
		ALA11	Alkyl, π-Alky	5.11				
		ILE112	Alkyl, π-Alky	4.70				
		PHE36	Alkyl, π-Alky	4.28				
3	−7.8	GLY23	Conventional H Bond	2.80	−8.1	LEU450	Conventional H Bond	3.07
		ALA11	C-H Bond	3.04		HIS227	π-π Stacked	5.36
		GLY23	π-Donor H Bond	3.43		TYR354	π-π Stacked	4.79
		MET25	π-Sigma	3.58		TYR225	π-π T-Shaped	4.33
		PHE36	π-Alky	4.62		PHE339	π-π T-Shaped	5.23
		ILE19	π-Alky	5.44,5.45		LEU350	Alkyl, π-Alky	5.41
		ALA115	π-Alky	5.28		ILE352	Alkyl, π-Alky	5.25
						VAL390	Alkyl, π-Alky	5.02
						PHE240	Alkyl, π-Alky	4.15
						PHE339	Alkyl, π-Alky	5.00
4	−7.9	TYR118	Conventional H Bond	2.09	−8.2	TYR354	π-Sulfur	5.82
		GLY23	Conventional H Bond	2.46		PHE339	π-π Stacked	5.68
		ALA11	C-H Bond	3.03		TYR225	π-π T-Shaped	4.63,5.50
		GLY23	π-Donor H Bond	3.51		TYR354	π-π T-Shaped	4.69
		MET25	π-Sigma	3.62		PHE240	π-Alkyl	4.85
		PHE36	π-Alkyl	4.85		HIS227	π-Alkyl	4.13
		ALA115	π-Alkyl	5.34		LEU394	π-Alkyl	4.52
		VAL10	π-Alkyl	5.40				
		ILE19	π-Alkyl	5.45,5.50				
5	−7.9	ILE112	Conventional H Bond	2.46,2.46	−8.1	LEU394	π-Sigma	4.66
		ILE9	Conventional H Bond	3.01		PHE339	π-Sulfur	5.71
		THR58	Conventional H Bond	2.20		TYR225	π-π Stacked	4.40
		GLY114	C-H Bond	3.66,3.71		VAL449	π-Alkyl	4.87
		MET25	π-Sigma	3.78,3.80		LEU394	π-Alkyl	4.72
		PHE36	π-π T-Shaped	3.73		LEU415	π-Alkyl	5.31
		TYR118	π-π T-Shaped	5.67				
		LEU69	Alkyl, π-Alky	5.08				
		ILE19	Alkyl, π-Alky	4.85				
		VAL10	Alkyl, π-Alky	5.49				
		PHE36	Alkyl, π-Alky	4.63				
6	−7.4	ILE9	Conventional H Bond	1.86	−8.2	ILE111	Conventional H Bond	2.64
		ILE112	Conventional H Bond	2.38		ASP110	Conventional H Bond	2.53
		ALA11	Conventional H Bond	2.20		ASP110	C-H Bond	3.43
		MET25	π-Sigma	3.85		TYR225	π-Sulfur	5.86
		PHE36	π-π Stacked	3.74		TYR225	π-π Stacked	3.70
		ILE62	Alkyl, π-Alky	3.97,4.51		PHE240	π-π T-Shaped	5.25
		LEU69	Alkyl, π-Alky	5.31		TYR354	π-π T-Shaped	5.47
						LEU394	Alkyl, π-Alky	4.10
						TYR225	Alkyl, π-Alky	5.06
7	−7.5	LYS24	Conventional H Bond	2.60	−8.2	LEU451	Conventional H Bond	2.79
		ILE112	C-H Bond	3.40		LEU451	π-Anion	4.32
		ILE9	C-H Bond	3.80		LEU394	π-Sigma	3.84
		MET25	π-Sigma	3.66,3.70		TYR119	π-Sulfur	5.90
		PHE36	π-π Stacked	3.79		PHE117	π-Sulfur	4.49
		LEU69	Alkyl, π-Alky	5.13		PHE117	π-π Stacked	4.51
		ILE19	Alkyl, π-Alky	4.91		TYR354	π-π T-Shaped	5.04
		PHE36	Alkyl, π-Alky	4.46		VAL449	Alkyl	4.98
						LEU394	Alkyl	4.65
8	−8	TYR118	Conventional H Bond	2.08	−8.9	HIS227	Conventional H Bond	2.38
		ILE19	Conventional H Bond	2.49		TYR354	π-Sulfur	5.30
		THR58	Conventional H Bond	2.59		TYR354	π-π Stacked	5.21
		SER61	Conventional H Bond	2.57		PHE240	π-π Stacked	4.89
		GLY27	Conventional H Bond	2.70		PHE115	π-π T-Shaped	4.91
		ALA11	C-H Bond	2.94		TYR225	π-π T-Shaped	3.73

(*continued on next page*)

Table 6 (*continued*)

Comp.	*C. albicans* DHFR (PDB: 4HOF)				*C. albicans* N-myristoyl transferase (PDB: 1IYL)			
	BA	Interacting residue	Type of interaction	Distance	BA	Interacting residue	Type of interaction	Distance
		GLY23	π-Donor H Bond	3.58		ILE352	Alkyl, π-Alky	4.83
		THR58	π-Donor H Bond	3.28		LEU350	Alkyl, π-Alky	4.78
		MET25	π-Sigma	3.57		VAL390	Alkyl, π-Alky	3.78
		PHE36	π-Alky	4.28		PHE240	Alkyl, π-Alky	4.01
		VAL10	π-Alky	5.44				

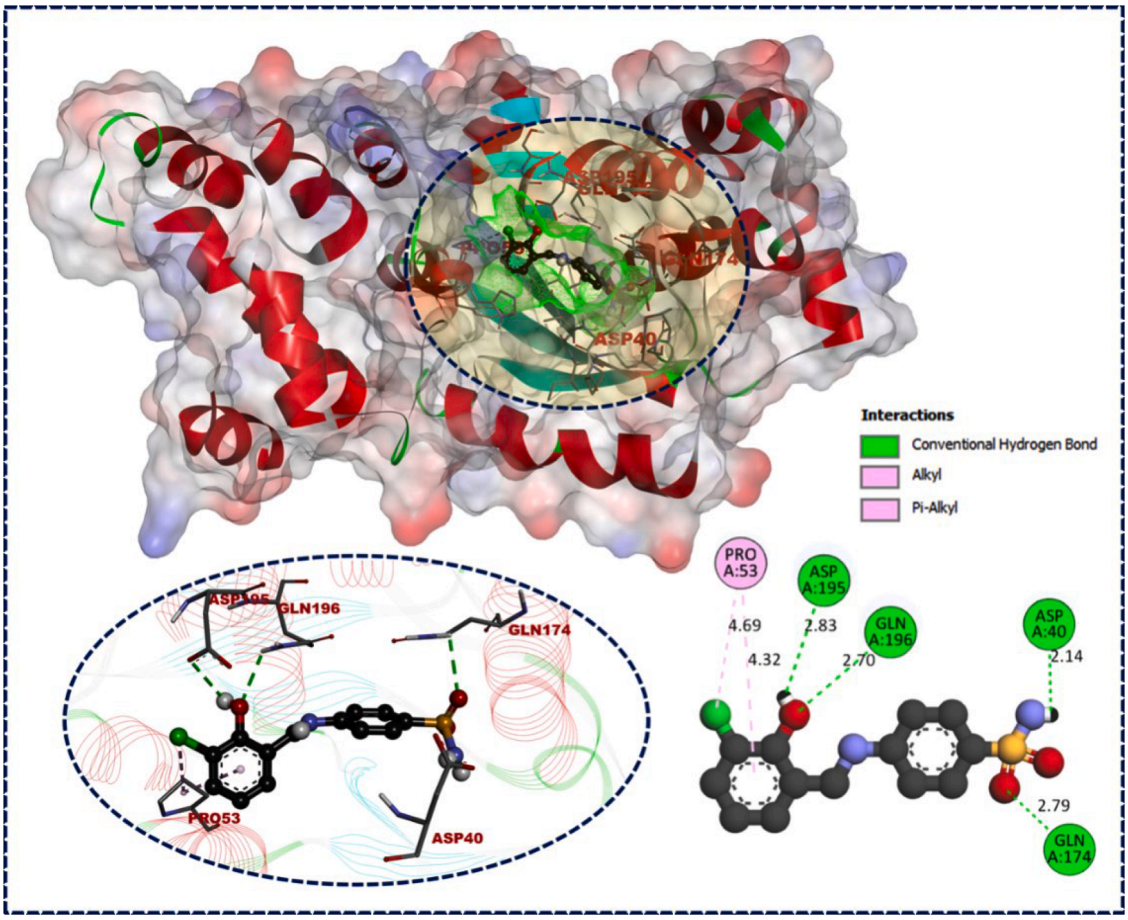

Fig. 3. Binding interaction of compound **8** against *S. aureus* TyrRS (PDB: 1JIJ).

emphasized the significance of evaluating the safety profile of title compounds. Pharmacokinetic profiling of title compounds provided valuable insights into their ADMET properties. *In-silico* assessment of drug-likeness and pharmacokinetic properties gives initial insights in molecules suitability as drug like candidate [36–41]. However, further optimization encompassing safety, efficacy, and specific targeted applications remain vital to propel these compounds towards successful drug candidates.

3.3. Molecular docking

The docking study was conducted against specific molecular targets from bacteria (*S. aureus*) and fungi (*C. albicans*) in order to predict the antibacterial and antifungal activities of the title compounds. The molecular targets selected for current investigation included TyrRS (PDB: 1JIJ) and DHRF (PDB: 3FYV) from *S. aureus* and DHFR (PDB: 4HOF) and N-myristoyl transferase (PDB: 1IYL) from *C. albicans*. The binding interactions and affinities of the compounds (**1–8**) against *S. aureus* TyrRS and DHRF are represented in Table 5, while Table 6 demonstrates binding interactions and affinities against DHFR and N-myristoyl transferase from *C. albicans*.

The binding affinity (BA) observed for the compounds were in the range of −7.4 kcal/mol to −8.7 kcal/mol against *S. aureus* TyrRS (PDB: 1JIJ). However, in comparison to the docked standard (**S1**) compound against *S. aureus* TyrRS, the BA of the compounds appeared relatively lower, given that the **S1** exhibited a higher BA of −11.1 kcal/mol. The discrepancy in BA between the title compounds and the **S1** against *S. aureus* TyrRS suggests differences in their respective binding strengths and interactions with the target protein. The compound **8** demonstrated the lowest negative BA (−8.7 kcal/mol) among the compounds studied via docking against *S. aureus* TyrRS. Notably, in the binding interaction analysis, compound **8** formed a total of four conventional hydrogen bonds with specific amino acid residues, namely ASP195, GLN196, ASP40, and GLN174. This interaction pattern suggests the formation of stable hydrogen bonds between compound **8** and the residues representing a favorable binding configuration and potential contribution to the strong binding affinity of the compound. Additionally, the binding interaction analysis revealed that PRO53 exhibited distinct types of interactions with compound **8**, primarily involving alkyl and π-alkyl interactions with *S. aureus* TyrRS. Fig. 3 illustrate the specific spatial

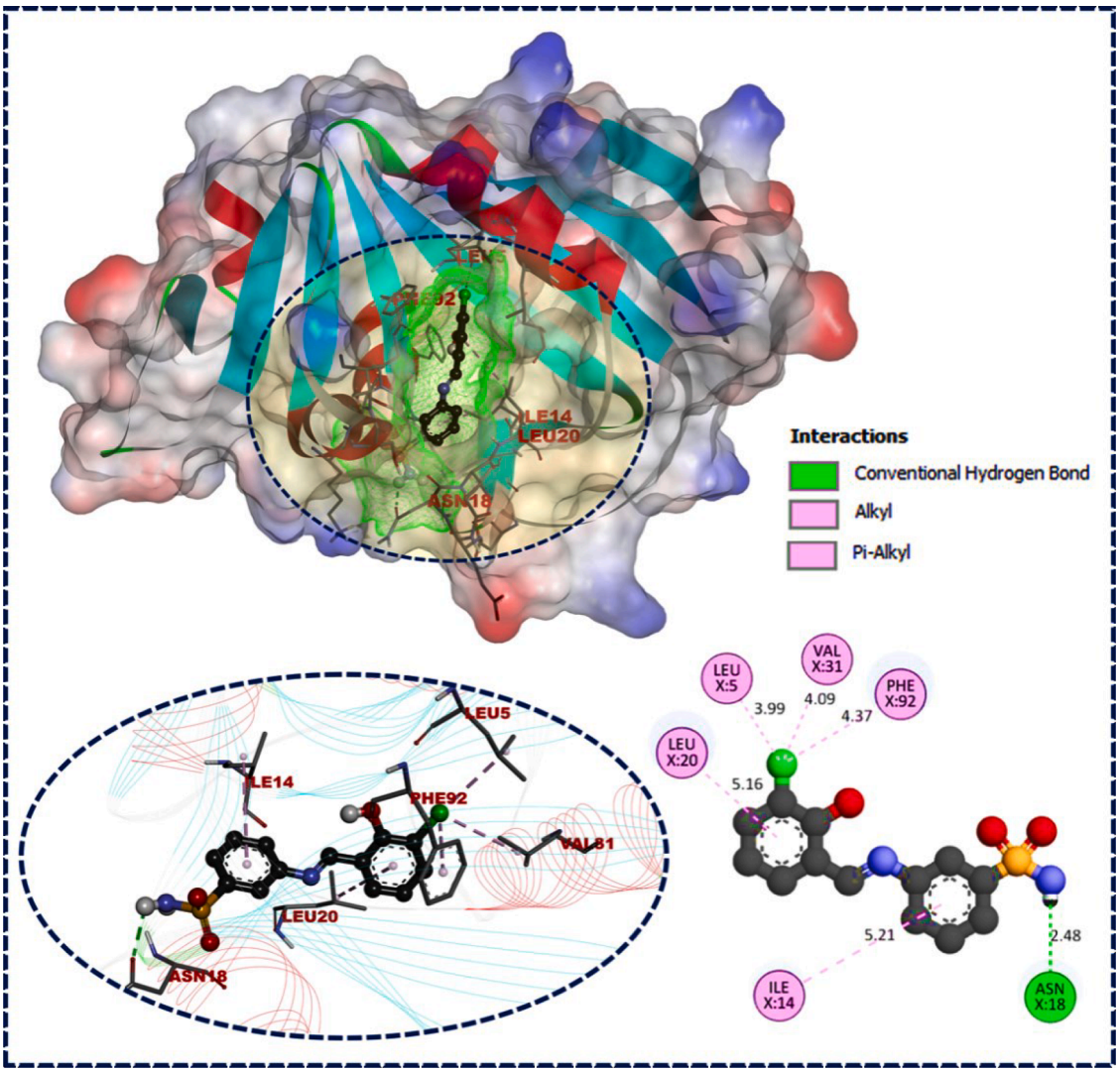

Fig. 4. Binding interaction of compound **2** against *S. aureus* DHFR (PDB: 3FYV).

arrangement and interactions between compound **8** and the amino acid residues within the binding pocket of *S. aureus* TyrRS. Compound **5** and **6** showed the BA of −8.5 kcal/mol and formed number of conventional hydrogen, charged, and hydrophobic interactions with *S. aureus* TyrRS. All the synthesized compounds shared interactions with almost identical residues within the binding sites of the *S. aureus* TyrRS. The 3D binding orientation of compounds, **1**–**8** and **S1** against *S. aureus* TyrRS are represented in **Supplementary Fig. S1-S9**.

The observed BA for the docked synthesized compounds against *S. aureus* DHFR (PDB: 3FYV) ranged from −8.1 kcal/mol to −8.5 kcal/mol. However, when compared to the BA of the docked **S1** against *S. aureus* DHFR, the synthesized compounds displayed relatively lesser binding affinities, with **S1** exhibiting a higher BA of −9.6 kcal/mol. This difference in BA between the synthesized compounds and **S1** against *S. aureus* DHFR denotes differences in their binding strengths and interactions with the targeted *S. aureus* DHFR. Among all the docked compounds against *S. aureus* DHFR, compound **2** showed the highest negative BA of −8.5 kcal/mol. This finding indicated that compound **2** exhibited the strongest binding interaction among the synthesized compounds with the *S. aureus* DHFR (PDB 3FYV). Relatively higher negative BA of compound **2** suggests its potential as a strong binder to the *S. aureus* DHFR compared to other docked synthesized compounds. This comparative analysis underscored compound **2** as a promising candidate among the synthesized compounds due to its higher BA with *S. aureus* DHFR (PDB 3FYV). In the binding interaction analysis of compound **2** with *S. aureus* DHFR (PDB 3FYV) indicated formation of a single conventional hydrogen bonds with ASN18 and five alkyl and π-alkyl interactions LEU20, PHE92, LEU5, VAL31, and ILE14from *S. aureus* DHFR. Fig. 4 illustrates the specific spatial arrangement and interactions between compound **2** and the amino acid residues within the binding pocket of *S. aureus* DHFR. The 3D binding orientation of compounds (**1**–**8**) and **S1** against *S. aureus* DHFR are represented in **Supplementary Fig. S10-S18**.

The resulting BA for the compounds ranging from −7.3 kcal/mol to -8 kcal/mol was observed against *C. albicans* DHFR (PDB: 4HOF). In comparison to the BA of the docked standard compound (**S2**) against *C. albicans* DHFR, the compounds displayed either equal or higher binding affinities as **S2** exhibited a BA of −7.3 kcal/mol. Among the compounds docked against *C. albicans* DHFR, compound **8** demonstrated the highest BA of -8 kcal/mol which is also higher compared to BA of **S2**. This indicated that compound **8** exhibited the strongest binding interaction among the title compounds with the *C. albicans* DHFR. Compound **8** exhibited the formation of a total of eight hydrogen bonds with *C. albicans* DHFR, comprising five conventional hydrogen bonds involving TYR118, ILE19, THR58, SER61, and GLY27, along with one carbon-hydrogen bond with ALA11 and two π-donor hydrogen bond with GLY23 and THR58. MET25 from *C. albicans* DHFR involved in formation of π-sigma interaction with the compound **8**. PHE36 and

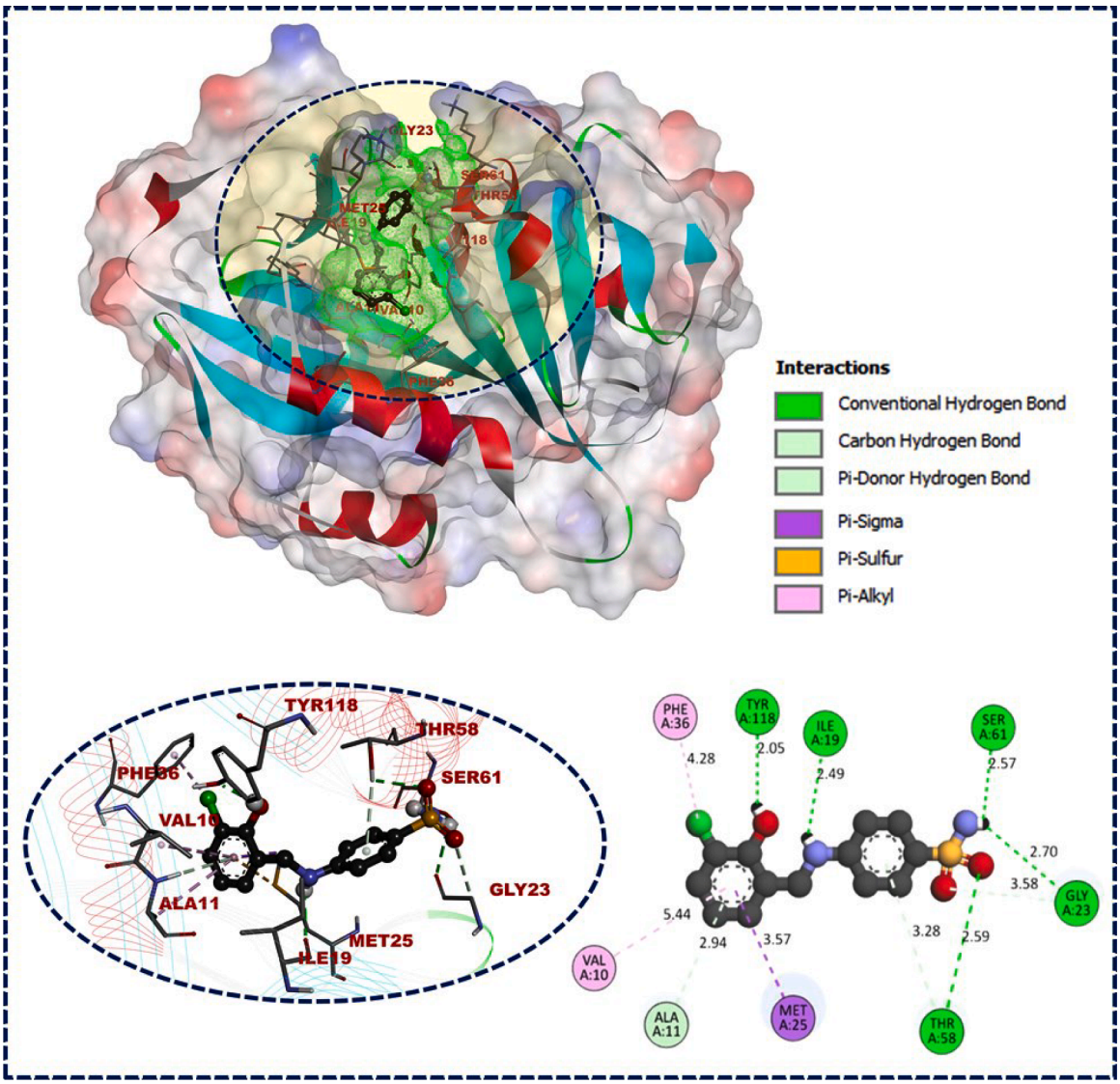

Fig. 5. Binding interaction of compound **8** against *C. albicans* DHFR (PDB: 4HOF).

VAL10 formed π-alky interaction with compound **8**. Fig. 5 represents binding interactions formed between compound **8** and *C. albicans* DHFR. The interactions between the synthesized compounds and *C. albicans* DHFR were consistent with involving highly similar residues. **Supplementary Fig. S19-S27** illustrates the 3D binding orientations of compounds (**1**–**8**) and **S2** in relation to *C. albicans* DHFR.

The synthesized compounds docked against *C. albicans* N-myristoyl transferase (PDB: 1IYL) showed BA ranging from −7.9 kcal/mol to −8.9 kcal/mol. Remarkably, the docked **S2** against *C. albicans* N-myristoyl transferase exhibited a BA of −8.9 kcal/mol. Compound **8** demonstrated the highest BA of −8.9 kcal/mol compared to other docked compounds against *C. albicans* N-myristoyl transferase. **S2** and compound **8** exhibited identical BA against *C. albicans* N-myristoyl transferase. This implies that compound **8** exhibited the strongest binding interaction among the tested compounds with the target protein which equivalent to the standard compound in terms of BA. Compound **8** established one conventional hydrogen bond with HIS227. Additionally, it formed a π-sulfur interaction with TYR354 and engaged in a π-π stacked interaction with TYR354 and TYR225. Furthermore, alkyl and π-alkyl interactions were observed with ILE352, LEU350, VAL390, and PHE240 from *C. albicans* N-myristoyl transferase. Fig. 6 depicts the binding interactions between compound **8** and the amino acid residues within the binding pocket of *C. albicans* N-myristoyltransferase. All the docked compound showed binding interactions with almost identical residues within the same binding site of the *C. albicans* N-myristoyl transferase. The 3D binding orientation of compounds (**1**–**8**) and **S2** against *C. albicans* N-myristoyl transferase are represented in **Supplementary Fig. S28-S36**.

The overall findings from the docking study performed against molecular targets of both bacteria and fungi aided in assessing the potential antibacterial and antifungal activities of the title compounds. This assessment was based on their binding affinities specifically observed with these molecular targets. Moreover, results of docking study provided structural insight into the interaction between the compounds and the selected molecular targets. Evaluating the binding interactions and affinities of the title compounds with these targets is crucial in predicting their antibacterial or antifungal potential against the respective bacterial and fungal species.

4. Conclusion

This research work utilizes both experimental laboratory studies and computational modeling techniques to comprehensively study the antibacterial and antifungal potential of some newer benzene sulfonamide derivatives. The experimental assays involved testing their antibacterial and antifingal activities against a range of bacterial and fungal

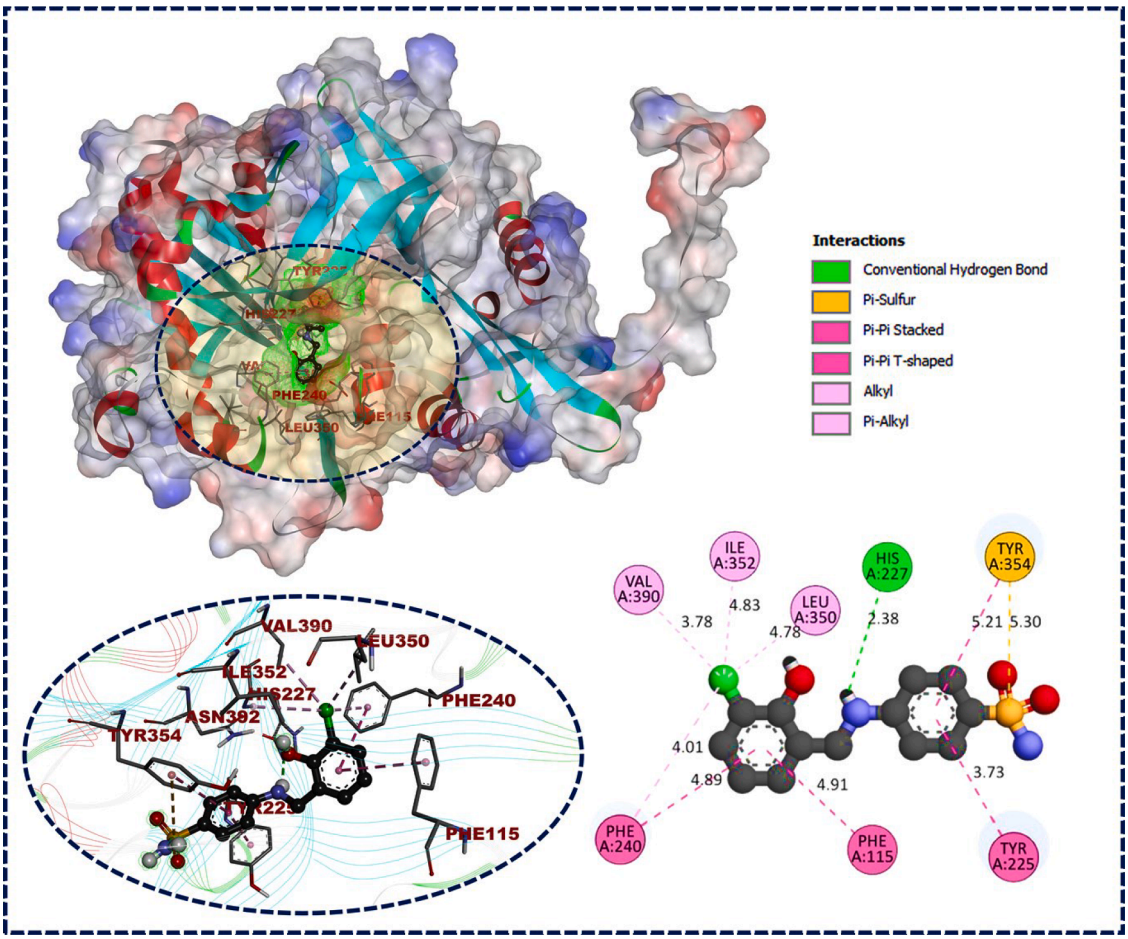

Fig. 6. Binding interaction of compound **8** against *C. albicans* N-myristoyl transferase (PDB: 1IYL).

strains. Concurrently, *in-silico* studies were utilized to predict the binding affinity and molecular interactions between benzene sulfonamides and bacterial or fungal targets, providing insights into their potential mechanisms of action as antimicrobial agents. The results of antibacterial/antifungal experiments substantiate the predictions made by computational studies and provide empirical evidence of antibacterial and antifungal potential of the reported benzene sulfonamide derivatives.

CRediT authorship contribution statement

Özge Kapısuz: Methodology, Investigation, Formal analysis, Data curation. **Mithun Rudrapal:** Writing – review & editing, Writing – original draft, Investigation, Project administration, Conceptualization. **Ülküye Dudu Gül:** Writing – original draft, Visualization, Methodology, Investigation, Data curation, Conceptualization. **Sanket S. Rathod:** Writing – original draft, Visualization, Validation, Formal analysis, Data curation. **Mesut Işık:** Writing – review & editing, Writing – original draft, Data curation, Supervision, Conceptualization. **Mustafa Durgun:** Writing – review & editing, Resources, Project administration. **Johra Khan:** Visualization, Validation, Funding acquisition.

Declaration of competing interest

The authors declare that they have no known competing financialinterestsor personal relationships that could have appeared to influence the work reported in this paper.

Data availability

No data was used for the research described in the article.

Supplementary materials

Supplementary material associated with this article can be found, in the online version, at doi:10.1016/j.chphi.2024.100712.

References

[1] G. Ozbey, E.S. Tanriverdi, B.F. Senkal, B. Korkmaz, S. Erkan, N. Bulut, B. Otlu, Investigation of antimicrobial activities and molecular docking studies of synthesized sulfonamide compounds, Pharmaceut. Chem. J. 57 (9) (2023) 1394–1400.
[2] I.R. Ezabadi, C. Camoutsis, P. Zoumpoulakis, A. Geronikaki, M. Soković, J. Glamočilija, A. Ćirić, Sulfonamide-1, 2, 4-triazole derivatives as antifungal and antibacterial agents: synthesis, biological evaluation, lipophilicity, and conformational studies, Bioorg. Med. Chem. 16 (3) (2008) 1150–1161.
[3] M. Mohamed, H. Abdelakder, B. Abdellah, Microwave assisted synthesis of 4-aminophenol Schiff bases: DFT computations, QSAR/Drug-likeness proprieties and antibacterial screening, J. Mol. Struct. 1241 (2021) 130666.
[4] A.M. Shawky, M.A. Abourehab, A.N. Abdalla, A.M. Gouda, Optimization of pyrrolizine-based Schiff bases with 4-thiazolidinone motif: design, synthesis and investigation of cytotoxicity and anti-inflammatory potency, Eur. J. Med. Chem. 185 (2020) 111780.
[5] F. Naaz, R. Srivastava, A. Singh, N. Singh, R. Verma, V.K. Singh, R.K. Singh, Molecular modeling, synthesis, antibacterial and cytotoxicity evaluation of sulfonamide derivatives of benzimidazole, indazole, benzothiazole and thiazole, Bioorg. Med. Chem. 26 (12) (2018) 3414–3428.
[6] P. Zoumpoulakis, C. Camoutsis, G. Pairas, M. Soković, J. Glamočlija, C. Potamitis, A. Pitsas, Synthesis of novel sulfonamide-1, 2, 4-triazoles, 1, 3, 4-thiadiazoles and 1, 3, 4-oxadiazoles, as potential antibacterial and antifungal agents. Biological

evaluation and conformational analysis studies, Bioorg. Med. Chem. 20 (4) (2012) 1569–1583.
[7] A.K. Bishoyi, M. Mahapatra, C.R. Sahoo, S.K. Paidesetty, R.N. Padhy, Design, molecular docking and antimicrobial assessment of newly synthesized p-cuminal-sulfonamide Schiff base derivatives, J. Mol. Struct. 1250 (2022) 131824.
[8] S. Kaya, S. Erkan, D. Karakaş, Computational investigation of molecular structures, spectroscopic properties and antitumor-antibacterial activities of some Schiff bases, SpectrochimicaActa Part A: Mol. Biomol. Spectrosc. 244 (2021) 118829.
[9] M. Durgun, C. Türkeş, M. Işık, Y. Demir, A. Saklı, A. Kuru, C.T. Supuran, Synthesis, characterisation, biological evaluation and in silico studies of sulphonamide Schiff bases, J. Enzyme Inhib. Med. Chem. 35 (1) (2020) 950–962.
[10] CLSI, Methods For Dilution Antimicrobial Susceptibility Tests For Bacteria That Grow Aerobically; Approved Standard, 9th Edition, Clinical and Laboratory Standards Institute, Wayne, Pennsylvania, USA, 2012. CLSI document M07-A9.
[11] A. Espinel-Ingroff, E. Cantón, Antifungal susceptibility testing of filamentous fungi. Antimicrobial Susceptibility Testing Protocols, CLSI, Wayne, PA, USA, 2007, pp. 209–241.
[12] A.E. Evren, S. Dawbaa, D. Nuha, S.A. Yavuz, Ü.D. Gül, L. Yurttaş, Design and synthesis of new 4-methylthiazole derivatives: in vitro and in silico studies of antimicrobial activity, J. Mol. Struct. 1241 (2021).
[13] E.J. Walsh, ACD/ChemSketch 1.0 (freeware); ACD/ChemSketch 2.0 and its Tautomers, Dictionary, and 3D Plug-ins; ACD/HNMR 2.0; ACD/CNMR 2.0, J ChemEduc 74 (1997).
[14] Advanced Chemistry Development Inc (ACD/Labs). ChemSketch (Freeware), version 2021 2.0 n.d.
[15] DassaultSystèmes. BIOVIA Discovery Studio Visualizer 2020.
[16] S. Choudhari, S.K. Patil, S. Rathod, Identification of hits as anti-obesity agents against human pancreatic lipase via docking, drug-likeness, in-silico ADME(T), pharmacophore, DFT, molecular dynamics, and MM/PB(GB)SA analysis, J Biomol. Struct.Dyn (2023) 1–23.
[17] N.M. O'boyle, M. Banck, C.A. James, C. Morley, T. Vandermeersch, G. R. Hutchison, Open Babel: an open chemical toolbox, J. Cheminform. 3 (2011) 1–14.
[18] A. Daina, O. Michielin, V. Zoete, SwissADME: a free web tool to evaluate pharmacokinetics, drug-likeness and medicinal chemistry friendliness of small molecules OPEN, Sci. Rep. 7 (2017) 42717.
[19] D.E.V. Pires, T.L. Blundell, D.B. Ascher, 1 ga UK. pkCSM: predicting Small-Molecule Pharmacokinetic and Toxicity Properties Using Graph-Based Signatures, J. Med. Chem. 58 (2015) 4066–4072.
[20] J. Neres, R.C. Hartkoorn, L.R. Chiarelli, R. Gadupudi, M.R. Pasca, G. Mori, et al., 2-carboxyquinoxalines kill mycobacterium tuberculosis through noncovalent inhibition of DprE1, ACS Chem.Biol 10 (2015) 705–714.
[21] X. Qiu, C.A. Janson, W.W. Smith, S.M. Green, P. McDevitt, K. Johanson, et al., Crystal structure of Staphylococcus aureus tyrosyl-tRNAsynthetase in complex with a class of potent and specific inhibitors, Protein Sci. 10 (2001) 2008–2016.
[22] C. Oefner, S. Parisi, H. Schulz, S. Lociuro, G.E. Dale, Inhibitory properties and X-ray crystallographic study of the binding of AR-101, AR-102 and iclaprim in ternary complexes with NADPH and dihydrofolate reductase from Staphylococcus aureus, Acta.Crystallogr D Biol.Crystallogr 65 (2009) 751–757.
[23] S. Sogabe, M. Masubuchi, K. Sakata, T.A. Fukami, K. Morikami, Y. Shiratori, et al., Crystal structures of Candida albicans N-myristoyltransferase with two distinct inhibitors, Chem.Biol 9 (2002) 1119–1128.
[24] N. G-Dayanandan, J.L. Paulsen, K. Viswanathan, S. Keshipeddy, M.N. Lombardo, W. Zhou, et al., Propargyl-linked antifolates are dual inhibitors of Candida albicans and Candida glabrata, J. Med. Chem. 57 (2014) 2643–2656.
[25] S. Rathod, K. Shinde, J. Porlekar, P. Choudhari, R. Dhavale, D. Mahuli, et al., Computational Exploration of Anti-cancer Potential of Flavonoids against Cyclin-Dependent Kinase 8: an In Silico Molecular Docking and Dynamic Approach, ACS. Omega 8 (2022) 391–409.
[26] A.G. Al-Sehemi, M. Pannipara, R.S. Parulekar, J.T. Kilbile, P.B. Choudhari, M. H. Shaikh, In silico exploration of binding potentials of anti SARS-CoV-1 phytochemicals against main protease of SARS-CoV-2, J. Saudi Chem. Soc. 26 (2022).
[27] J. Eberhardt, D. Santos-Martins, A.F. Tillack, S. Forli, AutoDockVina 1.2.0: new Docking Methods, Expanded Force Field, and Python Bindings, J ChemInf Model 61 (2021) 3891–3898.
[28] F. Stanzione, I. Giangreco, J.C. Cole, Use of molecular docking computational tools in drug discovery, Prog. Med. Chem. 60 (2021) 273–343.
[29] G. Corso, B. Jing, H. Stark, R. Barzilay, T. Jaakkola, Blind protein-ligand docking with diffusion-based deep generative models, Biophys. J. 122 (2023) 143a.
[30] S. Forli, R. Huey, M.E. Pique, M.F. Sanner, D.S. Goodsell, A.J. Olson, Computational protein-ligand docking and virtual drug screening with the AutoDock suite, Nat. Protoc. 11 (2016) 905–919.
[31] H.G. Aslan, S. Özcan, N &Karacan, The antibacterial activity of some sulfonamides and sulfonyl hydrazones, and 2D-QSAR study of a series of sulfonyl hydrazones, SpectrochimicaActa Part A: Mol. Biomol. Spectrosc. 98 (2012) 329–336.
[32] F.U. Eze, U.C. Okoro, D.I. Ugwu, S.N. Okafor, New carboxamides bearing benzenesulphonamides: synthesis, molecular docking and pharmacological properties, Bioorg. Chem. 92 (2019) 103265.
[33] C.Y. Jia, J.Y. Li, G.F. Hao, G.F. Yang, A drug-likeness toolbox facilitates ADMET study in drug discovery, Drug Discov. Today 25 (2020) 248–258.
[34] S. Rathod, D. Bhande, S. Pawar, K. Gumphalwad, P. Choudhari, H. More, Identification of potential hits against fungal lysine deacetylase rpd3 via molecular docking, molecular dynamics simulation, DFT, In-Silico ADMET and Drug-Likeness Assessment, Chemistry Africa (2023).
[35] H. van de Waterbeemd, E Gifford, ADMET in silico modelling: towards prediction paradise? Nat. Rev. Drug Discov. 2 (2003) 192–204, 2003 2:3.
[36] V.P. Archana, S.J. Armaković, S. Armaković, I. Celik, J.B. Bhagyasree, K.D. Babu, M. Rudrapal, I.S. Divya, R.R. Pillai, Exploring the structural, photophysical and optoelectronic properties of a diaryl heptanoid curcumin derivative and identification as a SARS-CoV-2 inhibitor, J. Mol. Struct. 1281 (2023) 135110.
[37] M. Rudrapal, K.K. Kirboga, M. Abdalla, S. Maji, Explainable artificial intelligence-assisted virtual screening and bioinformatics approaches for effective bioactivity prediction of phenolic cyclooxygenase-2 (COX-2) inhibitors using PubChem molecular fingerprints, Mol. Divers. 1-20 (2024).
[38] J.A. Ezugwu, U.C. Okoro, M.A. Ezeokonkwo, K.S. Hariprasad, M. Rudrapal, N. Gogoi, D. Chetia, D.I. Ugwu, F.U. Eze, L.E. Onyeyilim, C.C. Eze, Design, Synthesis, Molecular Docking, Drug-Likeness/ADMET and molecular dynamics studies of thiazolyl benzenesulfonamide carboxylates as antimalarial agents, Chem. Africa 1-6 (2024).
[39] K.D. Singh, D. Chetia, N. Gogoi, B. Gogoi, M. Rudrapal, In Vivo and in Silico based evaluation of antidiabetic potential of an isolated flavonoid from allium hookeri in type 2 diabetic rat model, Chem. Biodivers. 21 (1) (2024) e202301299.
[40] A. Paul, J.H. Zothantluanga, G. Rakshit, I. Celik, M. Rudrapal, M.K. Zaman, Computational Simulations Reveal the Synergistic Action of Phytochemicals of Morus alba to Exert Anti-Alzheimer Activity via Inhibition of Acetylcholinesterase and Glycogen Synthase Kinase-3β, Polycycl. Aromat. Compd. 1-25 (2023).
[41] R. Baru Venkata, D.S.N.B.K. Prasanth, P.K. Pasala, S.P. Panda, V.B. Tatipamula, S. Mulukuri, R.K. Kota, M. Rudrapal, J. Khan, S. Aldosari, B. Alshehri, Utilizing Andrographis paniculata leaves and roots by effective usage of the bioactive andrographolide and its nanodelivery: investigation of antikindling and antioxidant activities through in silico and in vivo studies, Front. Nutr. 10 (2023) 1185236.